Nov 7th, 12:00 AM - Nov 8th, 12:00 AM

Comparison of Experimental and Numerical Results for Flexural Capacity of Light-Gage Steel Roof Deck

Christopher H. Raebel

Dawid Gwodzdz

Wei-Wen Yu International Specialty Conference on Cold-Formed Steel Structures
St. Louis, Missouri, U.S.A., November 7 & 8, 2018

Comparison of Experimental and Numerical Results for Flexural Capacity of Light-Gage Steel Roof Deck

Christopher H. Raebel[1] and Dawid Gwozdz[2]

Abstract

The objective of this paper is to present a comparison between experimental results to each of two numerical analyses of cold formed steel roof deck in flexure. Prior numerical studies using the Direct Strength Method (DSM) and the Equivalent Width Method (EWM) have shown discrepancies between results obtained by the two methods. The goal of this research initiative was to compare results from each of the two numerical analysis methods to experimental results in an effort to determine which numerical method is most appropriate for analyzing steel deck in flexure.

Twenty-four physical tests were conducted using four different deck gages (22, 20, 18 and 16 gage) in both the deck's positive and negative positions. Detailed measurements of the physical geometry and the material properties of the deck samples were taken. Load was applied in a four-point bending scenario using a loading frame that engaged all flutes across the width of the deck sample. Deck was loaded to failure. Applied load and several displacement measurements were recorded. Maximum load measurements and load-displacement plots were used to determine the maximum moment capacity in the deck.

Finite strip modeling using CUFSM v4.03 was conducted and analyses using the DSM and EWM are compared to experimental results. It was found that the DSM and EWM vary in their prediction of the nominal moment capacity across material grades and deck thicknesses, but tend to converge to a constant ratio at higher deck gages. The EWM was found to be more accurate for thinner gages and the DSM was found to be more accurate for thicker gages, but both methods provide reasonable results when determining steel roof deck capacities.

[1] Associate Professor and Architectural Engineering Program Director, Milwaukee School of Engineering, Milwaukee, WI, USA. (corresponding author)
[2] Project Engineer, CSD Structural Engineers, Milwaukee, WI, USA.

Introduction

Light gage metal deck is often used in building construction. The versatility of the decking combined with its excellent strength-to-weight ratio makes it an attractive option as an integral element in typical roof and floor construction.

Roof deck is considered to be a structural component, meaning that it has the ability to support transverse and in-plane loading by means of resisting flexure, transverse shear and in-plane shear due to its inherent strength and stiffness. The deck is typically supported at multiple points along its length by joists or beams spaced at regular intervals beneath the deck. It is produced in a number of profiles, and each profile has its own advantages. The most common deck profile used in modern construction is wide rib (WR) deck, also commonly referred to as "Type B" deck. Wide rib deck has a well-balanced cross-sectional shape resulting in desirable structural properties. Wide rib deck can be attached to its supporting elements easily by means of mechanical fasteners or welds.

Roof deck is commonly produced using a carbon sheet steel conforming to ASTM A1008 or galvanized sheet steel conforming to ASTM A653. The yield stress for typical sheet steel materials is 33 ksi (227 MPa), but other yield stresses may be available and vary among manufacturers. Deck may be prime painted or galvanized.

Basic flexural capacities of standard roof deck can be calculated by straight-forward mechanics principles, and many manufacturers provide convenient design tables that incorporate these capacities. However, as the design becomes more optimized, the potential for several additional limit states arise. Of course, global bending will still occur and must be accounted for, but limit states such as local buckling, distortional buckling and lateral-torsional buckling may become prevalent in optimized designs.

The American Iron and Steel Institute (AISI) has embraced advanced analysis techniques that can aid designers and optimize designs. Two such methods, the Direct Strength Method (DSM) and Effective Width Method (EWM), can be used to analyze a variety of light-gage, cold-formed structural shapes including deck. These methods have become popular with designers, as they have shown to reflect accurate capacities for light-gage members.

The current research investigated the use of the DSM and EWM and compared numerical results to results obtained by means of experimental testing.

Project Origin and Recent Studies

A recent study by Dudenbostel (2015) investigated the use of the DSM and EWM for standard roof and floor deck. The study was limited to numerical analyses of roof and floor deck using geometric profiles and mechanical properties as reported in a manufacturer's design publication. Dudenbostel uncovered discrepancies between the numerical results as reported using the DSM and EWM when evaluating deck in flexure. The study concluded that additional research is necessary to determine which method best reports the flexural capacity of the deck.

No experimental testing was conducted as part of Dudenbostel's study, and no relevant test data was available for comparison. It was recommended that any future studies include experimental tests so that numerical results could be compared to results from in-situ testing.

Experimental Program

The experimental program included 24 full-scale tests of light-gage, wide rib roof deck. Four deck gages were considered: 22, 20, 18 and 16 gage. For each gage three tests were conducted in the deck's positive bending position (i.e., the typical position it would be in when resisting gravity loads when placed on the roof structure) and three tests were conducted in the negative bending position. The elastic section moduli differ between the top and bottom sections of the deck, so it was expected that the positive bending tests would yield somewhat different results than the negative bending tests.

The deck was tested in a four-point bending setup as illustrated in Figure 1. Each panel of deck was 3 ft (915 mm) wide, and the deck span between support points was 6 ft (1,830 mm). Applied loads were spaced at a 18 in. (458 mm) centered on the deck.

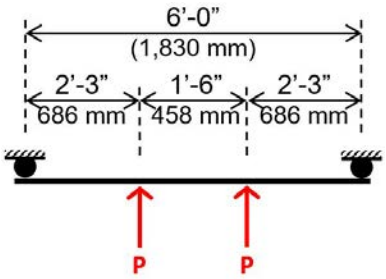

Figure 1. Schematic of four-point bending setup.

Load was applied by means of a hydraulic actuator pulling in the upward direction. The deck was loaded with a pulling force from the actuator to eliminate stability issues that typically arise when pushing with the hydraulic actuator. The load from the actuator was applied to the deck along two lines through a loading frame suspended from a load spreader beam by threaded rods.

The hydraulic actuators are instrumented with force and displacement transducers that measure in-line with the piston of the actuator. The loading frame, constructed of steel tube and being significantly stiffer than the light gage deck, applied lines of load orthogonal to the deck and uniformly across the deck. In addition to the displacement measurement taken by the actuator, four additional displacement readings were taken using Linear Variable Displacement Transducers (LVDTs) placed at the lines of applied loading near the edges of the deck. The five displacement measurements allowed for better understanding of the deformed shape of the deck up to and beyond the point of flexural yield and buckling. Figure 2 shows a pre-test photograph of the typical setup.

Part of the experimental program included material testing of the metal deck to discover its measured material properties. Two samples from each gage of deck, one from the flange and another from the flute, were tested by an independent and certified laboratory. The average measured tensile and yield strength magnitudes for each gage are summarized in Table 1.

Table 1. Measured material properties.

Property	**16 gage**	**18 gage**	**20 gage**	**22 gage**	**ASTM A1008**
Average Tensile Strength, psi (MPa)	54,500 (376)	52,250 (360)	54,250 (374)	57,000 (393)	52,000 (358)
Average Yield Strength, psi (MPa)	44,700 (308)	43,450 (300)	47,250 (326)	44,500 (307)	40,000 (276)

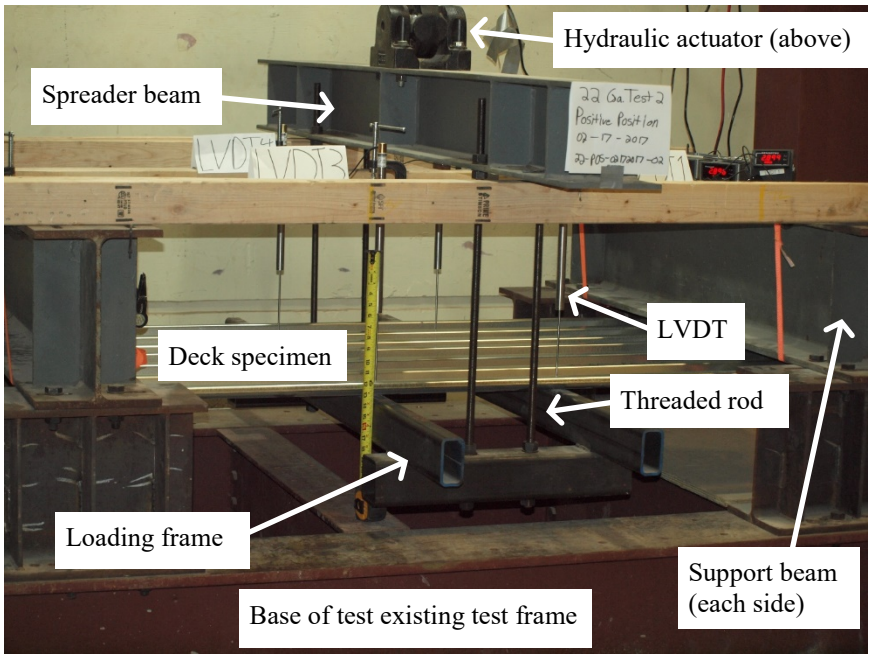

Figure 2. Typical Pre-test Configuration.

Experimental Results

Each test yielded force and displacement measurements read from the actuator's instrumentation and displacement measurements from each of the four LVDTs. Data is presented in force vs. displacement plots for each individual test.

Each of these plots clearly illustrated key ranges. Initially a force engagement range was observed, where the actuator lifted the load frame and deck specimen until the deck engaged its end supports. The force magnitude measured within the engagement range is the weight of the deck specimen, load frame, threaded rod, spreader beam and the actuator's bottom clevis. Next, a load accrual range occurred, where the deck was loaded slowly and continuously. The deck remained elastic during the load accrual range. Then, the deck reached its flexural peak and the maximum experimental moment was achieved. Local buckling was observed as the deck approached its maximum moment, as shown in Figure 3a. The initiation of local buckling was evident on the force versus displacement plots as the beginning of the nonlinear range prior to the maximum

applied force. Finally, the deck flutes buckled (Figure 3b) and the deck's flexural stiffness declined as did its moment resistance.

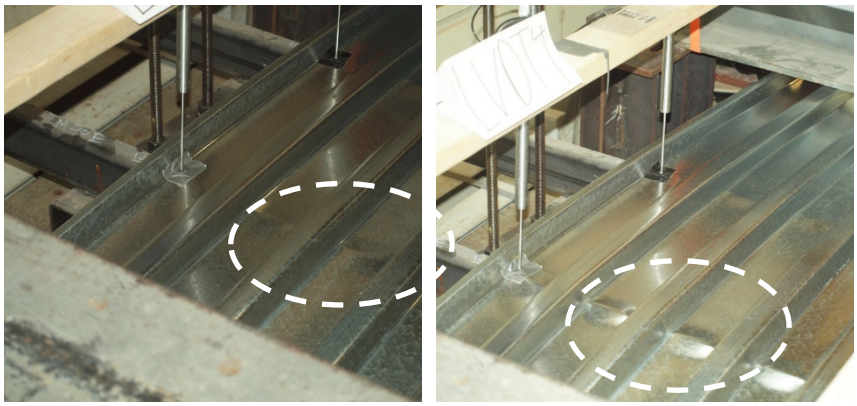

(a) Initial buckling between ribs. (b) Further buckling between ribs.

Figure 3. Local buckling of flange for a positive bending test.

Figures 4 and 5 show plots of applied force versus displacement measured by the actuator's displacement transducer. Key ranges are identified on the plots.

The nominal moment capacity, M_n, can be found using the yield force as measured from each specimen. Table 2 summarizes the average yield force and nominal moment capacity for each deck gage. The average weight of the specimen and fixtures, measured during the engagement range of each test, was subtracted from the maximum applied force in order to determine the yield force.

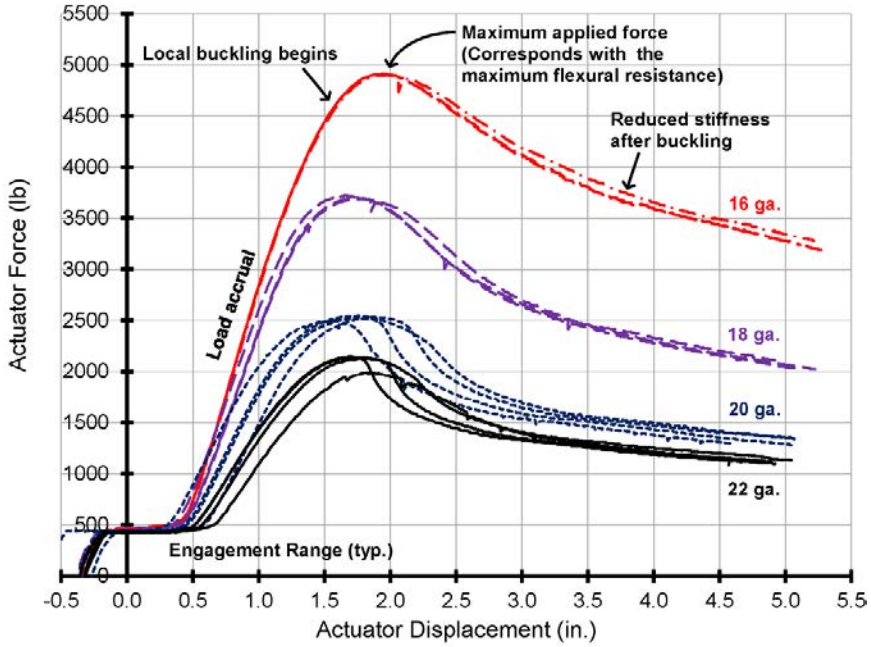

Figure 4. Actuator force vs. actuator displacement – all positive bending tests.

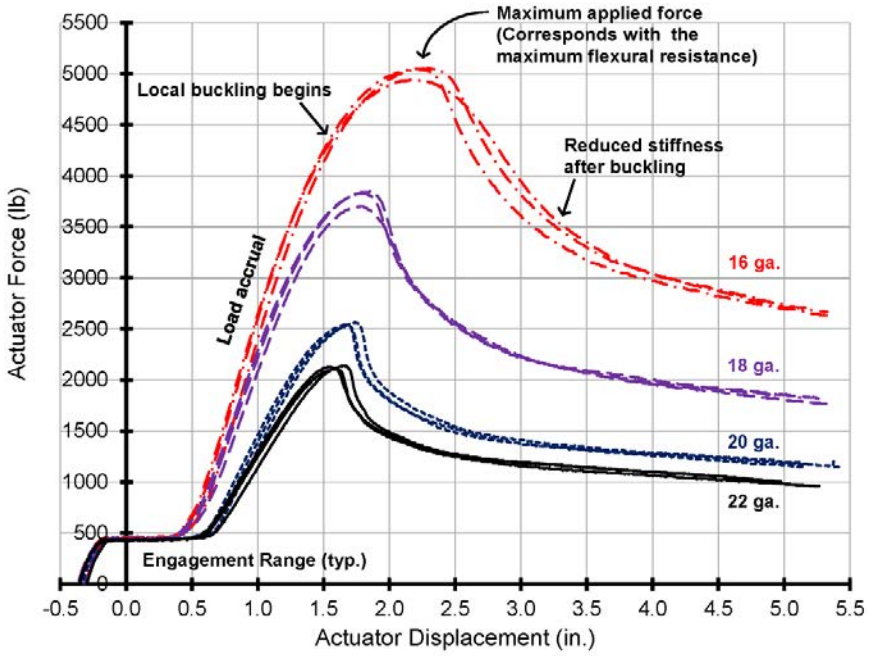

Figure 5. Actuator force vs. actuator displacement – all negative bending tests.

Table 2. Force and moment capacities – all tests.

Deck (Position)	Average Weight lb (kg)	Avg. Yield Force lb (N)	Nominal Moment lb-in. (N-m)
22 gage (Positive)	430 (195)	1,671 (7,433)	22,560 (2,549)
20 gage (Positive)	432 (196)	2,093 (9,310)	28,250 (3,192)
18 gage (Positive)	454 (206)	3,249 (14,452)	43,860 (4,956)
16 gage (Positive)	464 (210)	4,446 (19,780)	60,020 (6,781)
22 gage (Negative)	428 (194)	1,697 (7,549)	22,910 (2,588)
20 gage (Negative)	434 (197)	2,111 (9,390)	28,500 (3,220)
18 gage (Negative)	448 (203)	3,343 (14,870)	45,130 (5,099)
16 gage (Negative)	459 (208)	4,554 (20,260)	61,480 (6,946)

Numerical Analyses

Numerical analyses utilized the direct strength method and the equivalent width method. The measured material values were input to the numerical analyses in an effort to provide accurate comparisons to experimental results.

CUFSM v4.03 (Li and Schafer, 2010) was used to analyze the deck profile and develop the signature curve for each deck gage and bending position. The software utilizes the finite strip method to analyze a cross section based on user inputs of the geometry and material properties. The analysis begins with the user inputting nodes and attaching elements to the nodes such that the cross section will be an accurate representation of the actual deck profile. The user then inputs a stress distribution over the cross section based on the yield stress of the material. This could be a uniform distribution as found in tension or compression members or a linearly changing distribution typically found in flexural members.

The "half wavelengths" were input next, and they are important in determining the order of buckling failures. The half wavelengths were originally determined using a MATLAB preprocessor routine developed in prior research comparing the direct strength method and equivalent width method (Dudenbostel 2015). The software uses the length of the buckling failure that the cross section can exhibit and that the user wishes to consider. Enough half wavelengths are entered so the resulting signature curve displays the most accurate minimums. The signature curve is plotted using the half wavelengths and not having enough points can result in flat spots that miss the absolute minimum.

The final step in preparing the analysis is to input the base vectors. The base vectors are automatically generated in the software based on the cross section of the deck profile. The base vectors are required to normalize all of the different failures (local buckling, distortional buckling and global buckling) so they can be compared to one another in the signature curve and to determine which will control. The signature curve has minima, referred to as load factor, along the curve where a particular failure mode exists. The first minima corresponds with local buckling, the second minima corresponds with distortional buckling and the third minima corresponds with lateral torsional buckling. The load factors are used with the nominal moment equations for DSM (AISI 2012). Each deck thickness was analyzed using this method for bending in both the positive and negative orientation.

The equivalent width method (AISI 2012) was also used to find the nominal moment capacity. The deck profile was measured and input to AutoCAD, and the effective widths were determined based on the geometry. Each element's effective width is determined based on how it is connected to the other elements and whether or not it is stiffened. The widths then create a new set of section properties for the cross section that are used to calculate the point of local buckling, distortional buckling, global buckling and yielding. Each deck

thickness was analyzed using this method for bending in both the positive and negative orientation.

Discussion and Conclusions

Table 3 summarizes the experimental and numerical results as found using the DSM and EWM. The table also includes the yield moment, M_y, calculated manually.

Table 3. Summary of nominal moment capacities – all methods.

Deck	Exp. M_n lb-in. (N-m)	DSM M_n lb-in. (N-m)	EWM M_n lb-in. (N-m)	Yield M_y lb-in. (N-m)
22 gage (Positive)	22,560 (2,549)	16,670 [-26%] (1,883)	20,530 [-9%] (2,320)	25,370 [+12%] (2,866)
20 gage (Positive)	28,250 (3,192)	23,980 [-15%] (2,709)	27,660 [-2%] (3,125)	34,020 [+20%] (3,844)
18 gage (Positive)	43,860 (4,956)	37,930 [-14%] (4,286)	36,810 [-16%] (4,159)	41,710 [-5%] (4,713)
16 gage (Positive)	60,020 (6,781)	54,980 [-8%] (6,212)	50,380 [-16%] (5,692)	54,980 [-8%] (6,212)
22 gage (Negative)	22,910 (2,588)	20,530 [-10%] (2,320)	23,960 [-5%] (2,707)	25,370 [+11%] (2,866)
20 gage (Negative)	28,500 (3,220)	28,910 [+1%] (3,266)	32,290 [-13%] (3,648)	34,020 [+19%] (3,844)
18 gage (Negative)	45,130 (5,099)	40,220 [-11%] (4,544)	42,530 [-6%] (4,805)	41,710 [-8%] (4,713)
16 gage (Negative)	61,480 (6,946)	54,980 [-11%] (6,212)	55,410 [-10%] (6,260)	54,980 [-11%] (6,212)

Note: Percent difference from experimental value shown in square brackets.

The EWM provides comparable results to the experimental data for thinner gage deck specimens when subjected to bending in the positive position, whereas the DSM under predicts the capacity. Conversely, the EWM under predicts the nominal moment capacity for thicker deck specimens, but the DSM results in more comparable moment capacity predictions for thicker deck specimens and when the deck is in its positive position.

Both the EWM and DSM reasonably predict nominal moment capacity for deck subjected to negative bending, with percent differences of 13% or less when compared to experimental results. Stronger trends such as the one noted for positive bending were not observed.

As such, the EWM is the preferred method for thinner gage deck (20 gage or thinner) subjected to flexure and the DSM is preferred for thicker gage deck. The designer may choose to use the DSM in concert with CUFSM software for all cases. Doing so would be conservative, and CUFSM introduces computational efficiencies that may be attractive when analyzing roof deck.

Acknowledgments

This research initiative was supported by the Small Project Fellowship Program through the American Iron and Steel Institute. The Steel Deck Institute and National Roofing Contractor's Association also provided financial support. CANAM Steel donated the steel deck specimens used for experimental testing. The authors thank these organizations for their support.

The authors would also like to thank Dr. Tom Sputo, Dr. James Fisher, Mr. Joshua Buckholt and Mr. Randy Dudenbostel for their fruitful discussions and valuable input throughout the project.

References

AISI (2012). "North American Specification for the Design of Cold-Formed Steel Structural Members." AISI S100, American Iron and Steel Institute, Washington, D.C., USA.

Dudenbostel, R. (2015). "Direct Strength Method for Steel Deck." Master's Thesis, University of Florida, Ganesville, FL.

Dudenbostel, R., Sputo, T. and Schultz, W. (2015). "Direct Strength Method for Steel Deck." AISI-Specifications for the Design of Cold-Formed Steel Structural Members. 116.

Gwozdz, D. (2017). “Experimental and Numerical Comparison of Flexural Capacity of Light-Gage Cold Formed Steel Roof Deck.” Master’s Thesis, Milwaukee School of Engineering, Milwaukee, WI.

Li, Z. and Schafer, B.W. (2010). “Buckling Analysis of Cold-Formed Steel Members with General Boundary Conditions using CUFSM: Conventional and Constrained Finite Strip Methods.” Proceedings of the 20th Int’l. Spec. Conf. on Cold-Formed Steel Structures, St. Louis, MO.

Schafer, B.W. and Adany, S. (2006). “Buckling Analysis of Cold-Formed Steel Members using CUFSM: Conventional and Constrained Finite Strip Methods.” Proceedings of the 18th Int’l. Spec. Conf. on Cold-Formed Steel Structures, Orlando, FL.

Yu, C. and Lokie, T. (2006). “Effective Width Method Based Design for Distortional Buckling of Cold Formed Steel Beams.” Proceedings of the 18th Int’l. Spec. Conf. on Cold-Formed Steel Structures, Orlando, FL.